International Journal of Minerals, Metallurgy and Materials
Volume 19, Number 10, Oct 2012, Page 886
DOI: 10.1007/s12613-012-0643-x

Comparative study on the passivation layers of copper sulphide minerals during bioleaching

Kai-bin Fu[1,2], *Hai Lin*[1], *Xiao-lan Mo*[1], *Han Wang*[1], *Hong-wei Wen*[1], *and Zi-long Wen*[1]

1) School of Civil and Environmental Engineering, University of Science and Technology Beijing, Beijing 100083, China

2) Key Laboratory of Solid Waste Treatment and Resource Recycle (Ministry of Education), Southwest University of Science and Technology, Mianyang 621010, China

(Received: 11 October 2011; revised: 28 November 2011; accepted: 5 December 2011)

Abstract: The bioleaching of copper sulphide minerals was investigated by using *A. ferrooxidans* ATF6. The result shows the preferential order of the minerals bioleaching as djurleite>bornite>pyritic chalcopyrite>covellite>porphyry chalcopyrite. The residues were characterized by X-ray diffraction (XRD) and scanning electron microscopy (SEM). It is indicated that jarosite may not be responsible for hindered dissolution. The elemental sulfur layer on the surface of pyritic chalcopyrite residues is cracked. The compact surface layer of porphyry chalcopyrite may strongly hinder copper extraction. X-ray photoelectron spectroscopy (XPS) further confirms that the passivation layers of covellite, pyritic chalcopyrite, and porphyry chalcopyrite are copper-depleted sulphide Cu_4S_{11}, S8, and copper-rich iron-deficient polysulphide $Cu_4Fe_2S_9$, respectively. The ability of these passivation layers was found as $Cu_4Fe_2S_9$>Cu_4S_{11}>S_8>jarosite.

Keywords: copper ore treatment; copper sulphide; bioleaching; passivation

1. Introduction

The most successful copper heaping operations have been mainly applied in copper oxide minerals and secondary copper sulphide minerals [1]. The leaching rates of secondary copper sulphide minerals, such as chalcocite (Cu_2S) and covellite (CuS), are relatively high, and the bacterial heap leaching is practiced to recover copper from these minerals [2]. On the other hand, primary copper sulphide chalcopyrite ($CuFeS_2$), the most abundant copper mineral in the world, is also the most refractory mineral regarding chemical leaching as well as bioleaching [3-4]. The bioleaching of chalcopyrite is a key industry target [5]. The slow copper dissolution rate from chalcopyrite has been attributed to the formation of a passivation layer on the mineral surface [6]. The passivation layers, such as elemental sulfur [7-9], polysulphides [10], jarosites [11-13], and metal-deficient sulphides [14-15], may hinder further copper extraction by restricting the flow of bacteria, nutrients, oxidants, and reaction production to and from the mineral surface [16]. To tackle the problems of passivation or hindered dissolution, it is necessary to know about the passivation ability of these possible candidates for hindered dissolution.

The research presented here was intended to evaluate the ability of these passivation candidates to restrict copper sulphide minerals bioleaching using *A. ferrooxidans* ATF6. To perform this work, the bioleaching of djurleite, bornite, covellite, pyretic chalcopyrite, and porphyry chalcopyrite was investigated, X-ray diffraction (XRD) was used to identify the possible passivation candidates, the chemical composition and the morphological feature of leached residues were analyzed by scanning electron microscopy-energy dispersive spectra (SEM-EDS), and X-ray photoelectron spectroscopy (XPS) was used to identify elementals and their chemical states on the surfaces of mineral residues.

2. Materials and methods

2.1. Minerals

Five copper sulphide minerals were used in the experiments. These minerals included djurleite, bornite, covellite, pyritic chalcopyrite, and porphyry chalcopyrite, supplied by

Corresponding author: Hai Lin E-mail: linhai@ces.ustb.edu.cn

© University of Science and Technology Beijing and Springer-Verlag Berlin Heidelberg 2012

Bofang Copper Mine in Hunan Province, Dongxiang Copper Mine in Jiangxi Province, Zijinshan Copper Mine in Fujian Province, Lizhu Iron Mine in Zhejiang Province, and Dexing Copper Mine in Jiangxi Province, China, respectively. The chemical analysis of these minerals is shown in Table 1.

Table 1. Chemical analysis of copper sulphide minerals wt%

Minerals	Cu	Fe	S	Purity
Djurleite	71.94	1.22	20.53	90.65
Bornite	50.17	10.67	24.38	79.22
Covellite	60.26	3.20	33.52	90.48
Pyritic chalcopyrite	27.38	28.35	33.31	79.22
Porphyry chalcopyrite	27.88	28.29	32.36	80.62

XRD analysis showed djurleite ($Cu_{31}S_{16}$) with a small amount of chalcocite, bornite and quartz; bornite (Cu_5FeS_4) with a small amount of chalcopyrite, pyrite (FeS_2), helvite and quartz; covellite (CuS) with a small amount of pyrite and enargite; pyritic chalcopyrite ($CuFeS_2$) with a small amount of pyrite; and porphyry chalcopyrite ($CuFeS_2$) with a small amount of pyrite and quartz.

The handpicked samples were ground to small particles less than 74 μm in size using a porcelain ball mill. Samples were vacuum freeze-dried, and then sealed with nitrogen.

2.2. Bacterial strain used and growth conditions

The optimal cultivation conditions of *A. ferrooxidans* ATF6 are the temperature of 30°C, pH 2.0, and the rotation speed of 160 r/min. ATF6 was isolated from the acid mine water of a copper mine in Daye, Hubei Province, China, and then obtained through the different stages of domestication. The medium used for cell cultivation consisted of the following components (per litre) as $(NH_4)_2SO_4$ 2.0 g, K_2HPO_4 0.25 g, $MgSO_4{\cdot}7H_2O$ 0.25 g, KCl 0.1 g, and $FeSO_4{\cdot}7H_2O$ 44.2 g. The medium, without $FeSO_4$, was autoclaved at 112°C for 30 min. The $FeSO_4$ medium was sterilized through a 0.2 μm filter and was added aseptically to the iron free medium.

2.3. Bioleaching experiments

The copper sulphide minerals were pretreated in 250-mL flasks by a sulfuric acid solution (90 mL, pH 2). When the pH value was adjusted to 2, the nutrient and 10-mL inoculum were added to the flasks. The initial cell concentration was 1×10^6 cells·mL^{-1}. The mineral concentration was 2wt%. The flasks were kept at 30°C and shaken at 160 r/min. The number of viable bacteria, pH values, redox potential, and copper ion concentration in the leaching solution were determined at certain intervals. Distilled water was supplied to compensate the evaporation and maintain a solution volume of 100 mL in the flasks. The residues were washed with Milli-Q water, vacuum freeze-dried, and then sealed with nitrogen.

2.4. Analytical methods

The concentration of dissolved copper ions in the leaching solution was analyzed by atomic absorption spectrometry (AAS). The ferrous iron was determined by titration with potassium dichromate (K_2CrO_7). The pH value and redox potential were measured using an S20 SevenEasy pH/Eh process controller. The bacterial number was determined by blood cell counting chambers under a ZBM-300E biological microscope. The morphological feature and chemical composition of leached residues were analyzed using SEM and XRD. XPS was used for the surface analysis of each residue.

3. Results and discussion

3.1. Bioleaching of copper sulphide minerals

The test conditions were established first, and the optimal concentrations of initial ferrous ions ($[Fe^{2+}]_{initial}$) for djurleite, bornite, covellite, pyritic chalcopyrite, and porphyry chalcopyrite during bioleaching were 1.5, 0, 4.5, 4.5, and 1.5 g·L^{-1}, respectively. The bioleaching curves of copper sulphides in the presence of ATF6 are shown in Fig. 1.

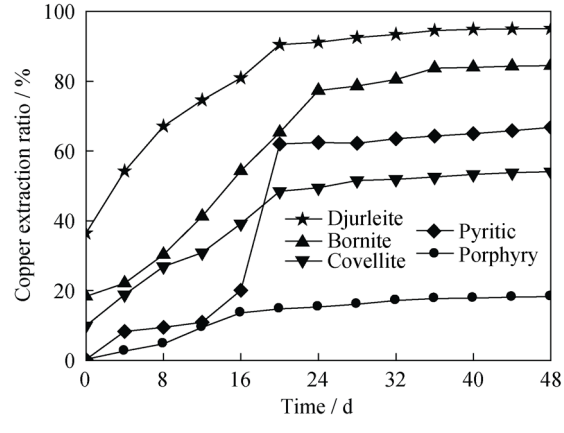

Fig. 1. Bioleaching curves of copper sulphides in the presence of ATF6 (30°C, 2wt% pulp density).

The pretreatment results in 36.45%, 18.38%, 9.92%, 0.28%, and 0.34% dissolution of djurleite, bornite, covellite, pyritic chalcopyrite, and porphyry chalcopyrite, respectively.

Fig. 1 shows that the copper extraction increases with the leaching time prolonging. After 48 d, the copper extraction ratios of djurleite, bornite, covellite, pyritic chalcopyrite, and porphyry chalcopyrite reach 95.12%, 84.5%, 54.1%, 66.77%, and 18.33%, respectively. The result indicates that the preferential order of copper sulphide minerals bioleaching is djurleite>bornite>pyritic chalcopyrite>covellite>porphyry chalcopyrite, which agrees with Ref. [17] by Dew *et al*. Generally, the slow dissolution of chalcopyrite results from the formation of a tenacious passivation layer [18-19]. It is supposed that a surface phase may restrict the dissolution of covellite.

3.2. XRD analysis

The residue XRD images of djurleite, bornite, covellite, pyritic chalcopyrite, and porphyry chalcopyrite are shown in Figs. 2-6, respectively.

Jarosite is characterized by monovalent cations, typically K^+, Na^+, H_3O^+, and NH_4^+, giving rise to potassium, sodium, hydronium, and ammonium jarosite [20]. XRD analysis confirms that jarosite is the main constituent of the leaching products of djurleite, bornite, and covellite, as shown in Figs. 2, 3 and 4(a). But djurleite and bornite are easily bio-oxidized, showing that jarosite does not restrain their bioleaching. Fig. 4 shows that ammoniojarosite is present in the covellite residues at $[Fe^{2+}]_{initial}$=4.5 g·L^{-1}, but is not found at $[Fe^{2+}]_{initial}$=0 g·L^{-1}; the corresponding copper extraction ratios for both the covellites are 54.1% and 52.8%, respectively. The result further indicates that jarosite may not be responsible for hindered dissolution. The precipitation of jarosite is thought to be an inevitable consequence of chalcopyrite during bioleaching [21]. However, the XRD analyses of two chalcopyrite residues can not detect jarosite, as shown in Figs. 5 and 6.

Cyclooctasulfur (S_8), a dominant stable solid sulphur allotrope [22], exists in the leach residues of djurleite and pyritic chalcopyrite in Figs. 2 and 5. Compared with jarosite, the content of S_8 in the djurleite bioleaching residues is rela-

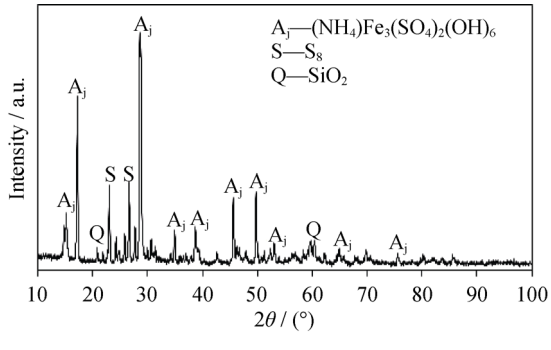

Fig. 2. XRD pattern of djurleite bioleaching residues at $[Fe^{2+}]_{initial}$=1.5 g·L^{-1}.

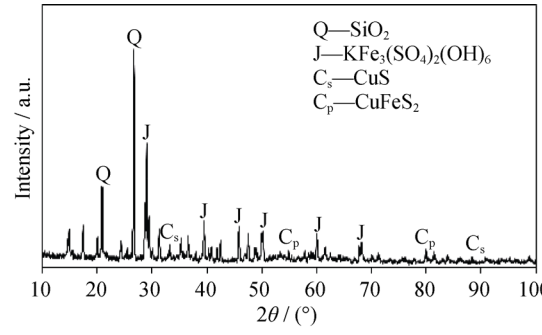

Fig. 3. XRD pattern of bornite bioleaching residues at $[Fe^{2+}]_{initial}$=0 g·L^{-1}.

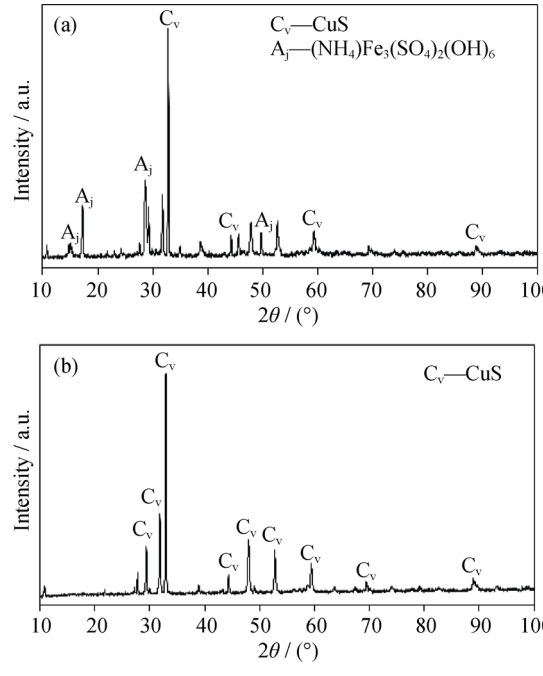

Fig. 4. XRD patterns of covellite bioleaching residues at $[Fe^{2+}]_{initial}$=4.5 g·L^{-1} (a) and 0 g·L^{-1} (b).

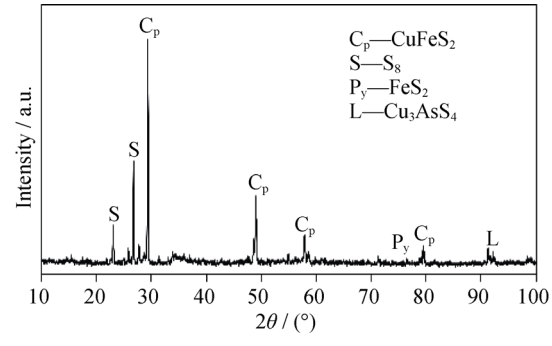

Fig. 5. XRD pattern of pyritic chalcopyrite bioleaching residues at $[Fe^{2+}]_{initial}$=4.5 g·L^{-1}.

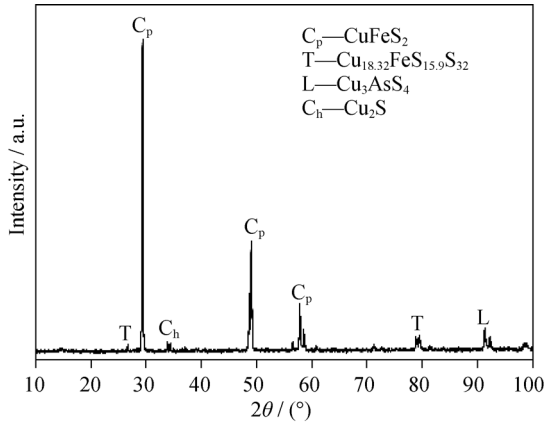

Fig. 6. XRD pattern of porphyry chalcopyrite bioleaching residues at $[Fe^{2+}]_{initial}$=1.5 g·L^{-1}.

tively less; the interactions of jarosite and S_8 may weaken the passivation ability of S_8. However, S_8 restrains the dissolution of pyritic chalcopyrite. The metal-deficient polysulphide $Cu_{18.32}Fe_{15.9}S_{32}$ is found in the bioleaching residues of porphyry chalcopyrite in Fig. 6, which may indicate that iron is preferentially leached to copper, and a characteristic surface phase, which is different from the bulk phase, forms on the surface of porphyry chalcopyrite residues.

3.3. SEM-EDS analysis

SEM images of djurleite bioleaching residues are shown in Fig. 7(a). The surface of djurleite is heavily etched and covered with a polyporous layer, which can not prevent the flow of bacteria, nutrients, oxidants and reaction production to and from the mineral surface. According to the corresponding EDS analysis in Fig. 7(b), Cu almost completely disappears; compared with the minerals before being oxidized, S and Fe obviously increase. The results reveal that djurleite is not limited in the presence of S_8 and jarosite.

Compared with djurleite, the low porosity of the residues surface layer may explain the poor results of bornite bioleaching in Fig. 8; EDS analysis of the residues further manifests that jarosite is formed.

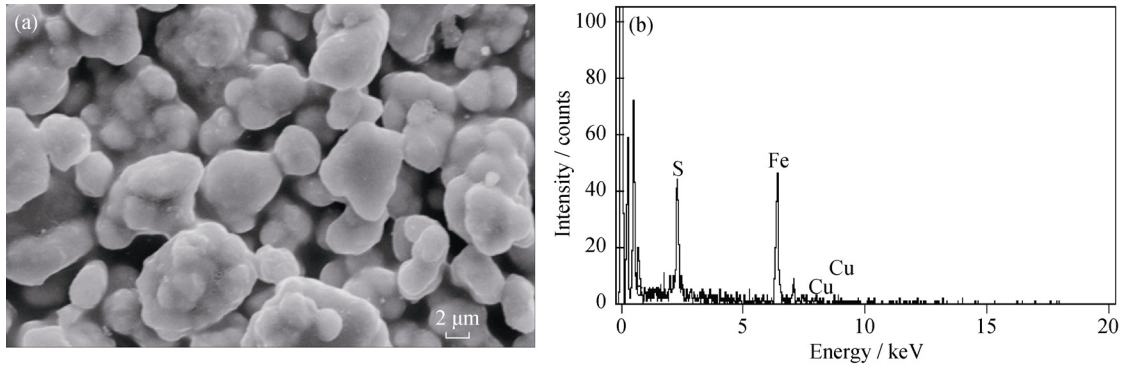

Fig. 7. SEM image (a) and EDS spectrum (b) of djurleite bioleaching residues.

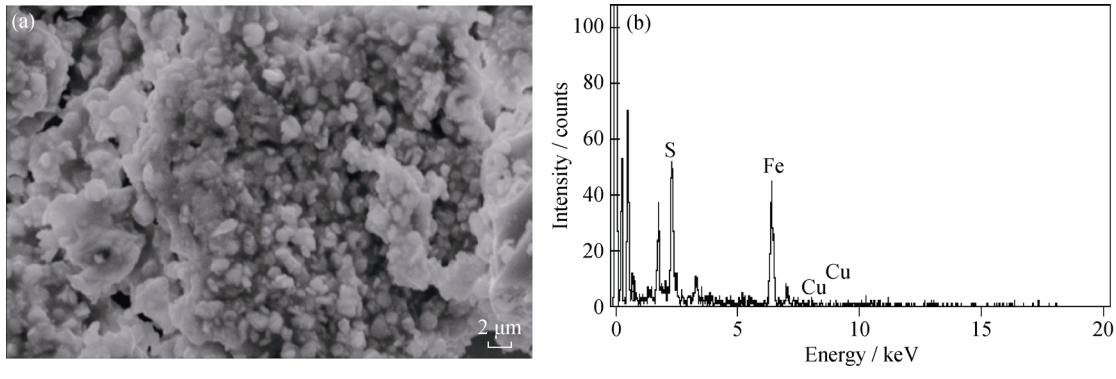

Fig. 8. SEM image (a) and EDS spectrum (b) of bornite bioleaching residues.

The SEM image and EDS spectrum of covellite bioleaching residues are given in Fig. 9. It can be seen that the surface of covellite bioleaching residues is cracked and holey. The EDS analysis indicates that the ratio of Cu/S on the surface of covellite bioleaching residues is different from that of covellite before being bio-oxidized. The result predicts the presence of a new phase on the surface of covellite bioleaching residues.

The surface of pyritic chalcopyrite bioleaching residues is cracked as shown in Fig. 10; the analyses of EDS and XRD reveal the formation of elemental sulphur. In contrast, the surface of porphyry chalcopyrite bioleaching residues is smooth and clear as shown in Fig. 11. The presence of a few small pits exhibits an insignificant dissolution feature. The compact layer may hinder the copper extraction strongly for porphyry chalcopyrite.

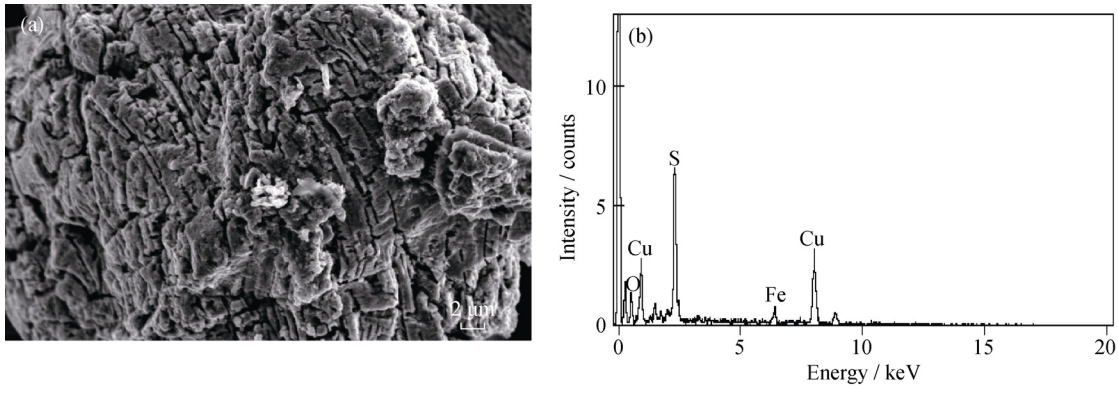

Fig. 9. SEM image (a) and EDS spectrum (b) of covellite bioleaching residues at $[Fe^{2+}]_{initial}$=0 g·L^{-1}.

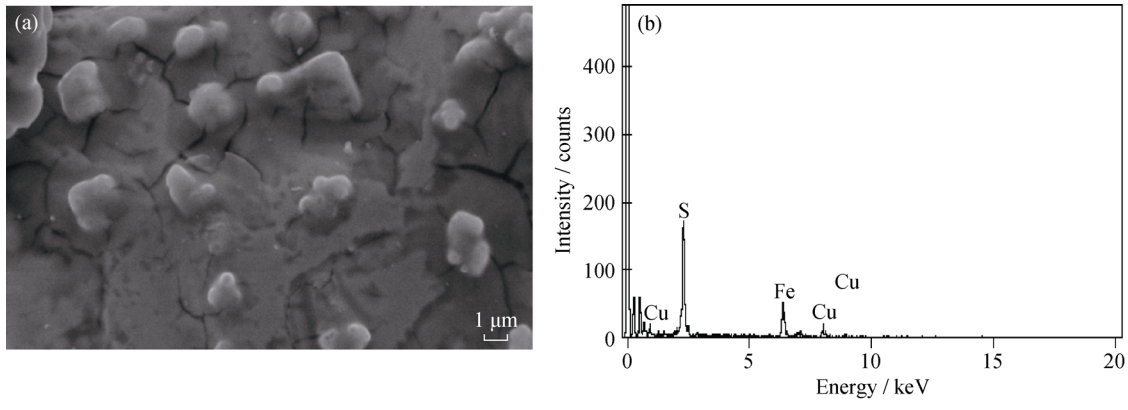

Fig. 10. SEM image (a) and EDS spectrum (b) of pyritic chalcopyrite bioleaching residues.

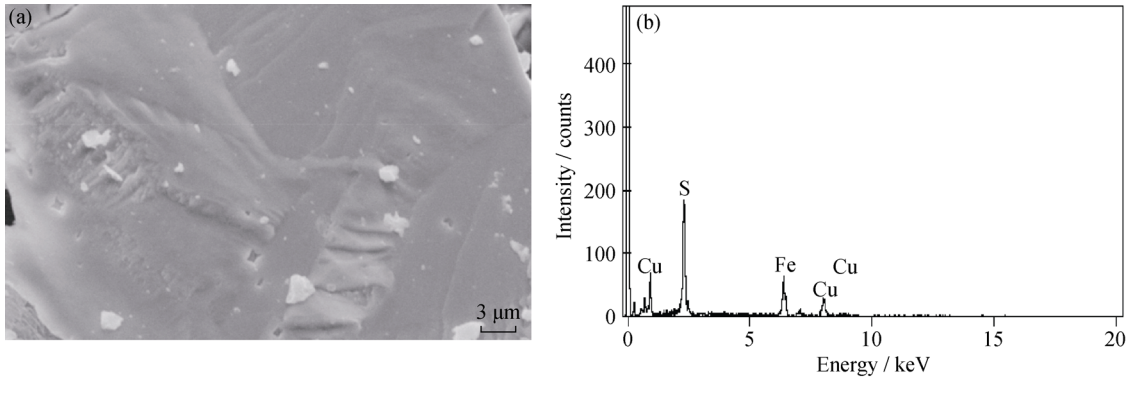

Fig. 11. SEM image (a) and EDS spectrum (b) of porphyry chalcopyrite bioleaching residues.

3.4. XPS analysis

XPS is singularly powerful in giving the direct information of surface phases and can be used to identify elements and their chemical state on the surface of copper sulphide bioleaching residues [23]. The spectra of Cu2p, Fe2p, and S2p are given in Fig. 12. The atomic fractions of Cu, Fe, and S present on the surface of residues are listed in Table 2.

Table 2 shows that 0% Cu, 19.74% Fe, and 80.26% S are present on the surface of pyritic chalcopyrite bioleaching residues, which indicates that the residues surface is mainly

covered by elemental sulfur (163.7 eV), So, Cu is very difficult to be detected by XPS, as shown in Fig. 12(a). The pyritic chalcopyrite bioleaching residues has a weak peak at 711.8 eV, which indicates that Fe(II) in chalcopyrite is oxidized to Fe(III) [24], and a minor amount of Fe(III) adheres to the surface of elemental sulfur. The passivation layer for pyritic chalcopyrite consists of elemental sulfur S^0 (163.7 eV).

In comparison with the theoretical value for $CuFeS_2$, the bioleaching results in a significant increase of Cu and S and a decrease of Fe in the porphyry chalcopyrite bioleaching residues, as shown in Table 2. This demonstrates the preferential bio-oxidation of iron. The Cu2p spectrum of the porphyry chalcopyrite bioleaching residues shows a formation of Cu(I)-containing species with $Cu2p_{3/2}$ component at 932.2 eV. The Fe2p spectrum shows the increase of Fe(III) at 711.8 eV, and the decrease of Fe(II) at 708.8 eV on the surface of the porphyry chalcopyrite bioleaching residues. The S2p spectrum of porphyry chalcopyrite bioleaching residues is shown in Fig. 12(c). The fitted S2p doublets are in good agreement with those reported by Parker *et al.* [10], which indicated sulphide (S^{2-}) from Cu_2S with a binding energy of $S2p_{3/2}$ 161.7eV and disulphide (S_2^{2-}) from a metal deficient surface phase of chalcopyrite at 162.7 eV. The evidence supports that the film "copper-enriched iron-depleted polysulphide" $Cu_4Fe_2S_9$ forms on the surface of porphyry chalcopyrite bioleaching residues, $Cu_4Fe_2S_9$ is composed of Cu^+, Fe^{3+}, $S^{2-}$and S_2^{2-}

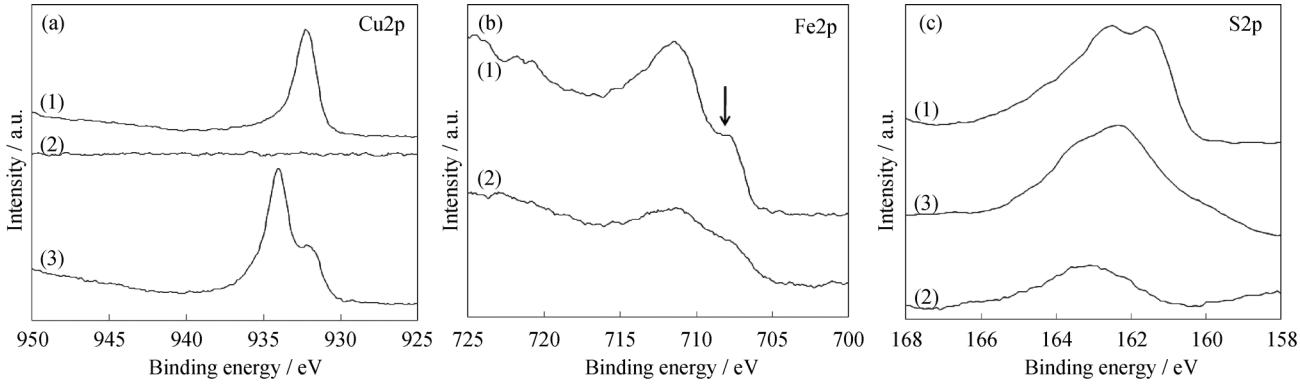

Fig. 12. Cu2p (a), Fe2p (b), and S2p (c) photoelectron spectrum for the residue surfaces of covellite (3), pyritic chalcopyrite (2), and porphyry (1) chalcopyrite.

Table 2. Atomic fractions of Cu, Fe, and S present on the bioleaching residue surfaces of covellite, pyritic chalcopyrite, and porphyry chalcopyrite **at%**

Minerals	Cu	Fe	S
Porphyry chalcopyrite	27.00	13.13	59.87
Covellite	26.67	0	73.33
Pyritic chalcopyrite	0	19.74	80.26

CuS contains both Cu(I) and Cu(II), and is assumed to be $Cu_2^{I}S \cdot Cu^{II}S_2$; the adsorption peaks of S_2^{2-} and S^{2-} are at 160.9 and 161.71 eV, respectively [25]. Todd *et al.* [24] regarded the leading adsorption peak at 932.2 eV as arising from Cu(II) bonded to sulfur and the small shoulder near 934.7 eV as arising from Cu(I) in the sulfide lattice at the surface of pristine covellite. The S2p spectrum of covellite shows that an absorption peak from Cu(I) (934.7 eV) is more intense than that from Cu(II) (932.2 eV); the reason for this is that Cu(I) is oxidized to Cu(II). The $S2p_{3/2}$ spectrum shifts to a binding energy of 163.0 eV, which can be attributed to the formation of S_n^{2-} for the $[Cu(I)_3(S_4)_3]^{3-}$ sample [26]. The ratios Cu/S for the residues in Table 2 allows us to conclude that a copper-depleted sulphide layer, Cu_4S_{11}, is responsible for hindered dissolution of covellite.

Therefore, according to the analyses of copper leaching rates, SEM-EDS, and XPS, the ability of three passivation layers is as the following: copper-rich iron-deficient polysulphide, $Cu_4Fe_2S_9$>copper-deficient sulphide, Cu_4S_{11}>elemental octasulfur, S_8.

4. Conclusions

(1) Porphyry chalcopyrite is the most refractory mineral. The preferential order of copper sulphide minerals bioleaching is djurleite>bornite>pyritic chalcopyrite>covellite>porphyry chalcopyrite.

(2) XRD analysis confirms that jarosite is the main constituent in the leaching products of djurleite, bornite, and covellite. But the three minerals bioleaching yields indicate that jarosite may not be responsible for hindered dissolution. No jarosite is detected in the two chalcopyrite bioleaching residues.

(3) Jarosite is polyporous, and cannot restrain the bioleaching of djurleite and bornite. The surface of covellite bioleaching residues is cracked and holey. In contrast, an elemental sulfur layer on the surface of pyritic chalcopyrite bioleaching residues is less cracked. The surface of porphyry chalcopyrite bioleaching residues is smooth and clear; the compact layer may hinder the porphyry chalcopyrite bioleaching.

(4) XPS shows that the passivation layers of covellite, pyritic chalcopyrite, and porphyry chalcopyrite are copper-depleted sulphide Cu_4S_{11}, elemental octasulfur S_8, and copper-enriched iron-depleted polysulphide $Cu_4Fe_2S_9$, respectively.

(5) According to the analyses of copper leaching rate, SEM-EDS, and XPS, it is easy to find that the ability of these passivation layers is $Cu_4Fe_2S_9$>Cu_4S_{11}>S_8>jarosite.

References

[1] H.R. Watling, The bioleaching of sulphide minerals with emphasis on copper sulphides: a review, *Hydrometallurgy*, 84(2006), No.1-2, p.81.

[2] H.L. Ehrlich, Past, present and future of biohydrometallurgy, *Hydrometallurgy*, 59(2001), No.2-3, p.127.

[3] E.M. Arce and I. González, A comparative study of electrochemical behavior of chalcopyrite, chalcocite and bornite in sulphuric acid solution, *Int. J. Miner. Process.,* 67(2002), No.1-4, p.17.

[4] K.B. Fu, H. Lin, X.L. Mo, Y.B. Dong, and L. Zhou, Study on bioleaching of different types of chalcopyrite, *J. Univ. Sci. Technol. Beijing*, 33(2011), No.7, p.806.

[5] D. Dreisinger, Copper leaching from primary sulfides: options for biological and chemical extraction of copper, *Hydrometallurgy*, 83(2006), No.1-4, p.10.

[6] E.M. Córdoba, J.A. Muñoz, M.L. Bláquez, F. González, and A. Ballester, Passivation of chalcopyrite during its chemical leaching with ferric ion at 68°C, *Miner. Eng.*, 22(2009), No.3, p.229.

[7] J.E. Dutrizac, Elemental sulphur formation during the ferric sulphate leaching of chalcopyrite, *Can. Metall. Q.*, 28(1989), No.4, p.337.

[8] C. Klauber, A. Parker, W. Van Bronswijk, and H. Watling, Sulphur speciation of leached chalcopyrite surfaces as determined by X-ray photoelectron spectroscopy, *Int. J. Miner. Process.*, 62(2001), No.1-4, p.65.

[9] D. Bevilaqua, I. Diéz-Perez, C.S. Fugivara, F. Sanz, A.V. Benedetti, and O. Garcia Jr., Oxidative dissolution of chalcopyrite by *Acidithiobacillus ferrooxidans* analyzed by electrochemical impedance spectroscopy and atomic force microscopy, *Bioelectrochemistry*, 64(2004), No.1, p.79.

[10] A.J. Parker, R.L. Paul, and G.P. Power, Electrochemistry of the oxidative leaching of copper from chalcopyrite, *J. Electroanal. Chem.*, 118(1981), p.305.

[11] A. Parker, C. Klauber, A. Kougianos, H.R. Watling, and W. Van Bronswijk, An X-ray photoelectron spectroscopy study of the mechanism of oxidative dissolution of chalcopyrite, *Hydrometallurgy*, 71(2003), No.1-2, p.265.

[12] A. Sandström, A. Shchukarev, and J. Paul, XPS characterisation of chalcopyrite chemically and bio-leached at high and low redox potential, *Miner. Eng.*, 18(2005), No.5, p.505.

[13] K.A. Third, R. Cord-Ruwisch, and H.R. Watling, Role of iron-oxidizing bacteria in stimulation or inhibition of chalcopyrite bioleaching, *Hydrometallurgy*, 57(2000), No.3, p.225.

[14] P. Acero, J. Cama, and C. Ayora, Kinetics of chalcopyrite dissolution at pH 3, *Eur. J. Mineral.*, 19(2007), No.2, p.173.

[15] K.B. Fu, H. Lin, X.L. Mo, Y.B. Dong, and H. Wang, Passivation of different genetic types of chalcopyrite bioleaching, *J. Cent. South Univ. Sci. Technol.*, 42(2011), No.11, p.3245.

[16] R.P. Hackl, D.B. Dreisinger, E. Peters, and J.A. King, Passivation of chalcopyrite during oxidative leaching in sulfate media, *Hydrometallurgy*, 39(1995), No.1-3, p.25.

[17] D.W. Dew, C. Van Buuren, K. Mcewan, and C. Bowker, Bioleaching of base metal sulphide concentrates: A comparison of mesophile and thermopile bacterial cultures, [in] *13th International Biohydrometallurgy Symposium IBS'99*, Madrid, 1999, p.229.

[18] F.B. Mateos, I.P. Pérez, and F.C. Mora, The passivation of chalcopyrite subjected to ferric sulphate leaching and its reactivation with metal sulphides, *Hydrometallurgy*, 19(1987), No.2, p.159.

[19] T. Biegler and M.D. Horne, Electrochemistry of surface oxidation of chalcopyrite, *J. Electrochem. Soc.*, 132(1985), No.6, p.1363.

[20] J.Y. Liu, X.X. Tao, and P. Cai, Study of formation of jarosite mediated by *Thiobacillus ferrooxidans* in 9K medium, *Procedia Earth. Planet. Sci.*, 1(2009), No.1, p.706.

[21] J.E. Dutrizac, The effect of seeding on the rate of precipitation of ammonium jarosite and sodium jarosite, *Hydrometallurgy*, 42(1996), No. 3 p.293.

[22] B. Meyer, Elemental sulfur, *Chem. Rev.*, 76(1976), No.3, p.367.

[23] C. Klauber, A critical review of the surface chemistry of acidic ferric sulphate dissolution of chalcopyrite with regards to hindered dissolution, *Int. J. Miner. Process.*, 86(2008), No.1-4, p.1.

[24] E.C. Todd, D.M. Sherman, and J.A. Purton, Surface oxidation of chalcopyrite ($CuFeS_2$) under ambient atmospheric and aqueous (pH 2-10) conditions: Cu, Fe L- and O K-edge X-ray spectroscopy, *Geochim. Cosmochim. Acta*, 67(2003), No.12, p.2137.

[25] S.W. Goh, A.N. Buckley, R.N. Lamb, R.A. Rosenberg, and D. Moran, The oxidation states of copper and iron in mineral sulfides, and the oxides formed on initial exposure of chalcopyrite and bornite to air, *Geochim. Cosmochim. Acta*, 70(2006), No.9, p.2210.

[26] S.L. Harmer, *Surface Layer Control for Improved Copper Recovery for Chalcopyrite Leaching* [Dissertation], University of South Australia, Adelaide, 2002.